

Search for Excited Electrons at HERA

H1 Collaboration

Abstract

A search for excited electron (e^*) production is described in which the electroweak decays $e^* \rightarrow e\gamma$, $e^* \rightarrow eZ$ and $e^* \rightarrow \nu W$ are considered. The data used correspond to an integrated luminosity of 120 pb^{-1} taken in $e^\pm p$ collisions from 1994 to 2000 with the H1 detector at HERA at centre-of-mass energies of 300 and 318 GeV. No evidence for a signal is found. Mass dependent exclusion limits are derived for the ratio of the couplings to the compositeness scale, f/Λ . These limits extend the excluded region to higher masses than has been possible in previous direct searches for excited electrons.

To be submitted to
Physics Letters B

C. Adloff³³, V. Andreev²⁴, B. Andrieu²⁷, T. Anthonis⁴, A. Astvatsatourov³⁵, A. Babaev²³,
 J. Bähr³⁵, P. Baranov²⁴, E. Barrelet²⁸, W. Bartel¹⁰, S. Baumgartner³⁶, J. Becker³⁷,
 M. Beckingham²¹, A. Beglarian³⁴, O. Behnke¹³, A. Belousov²⁴, Ch. Berger¹, T. Berndt¹⁴,
 J.C. Bizot²⁶, J. Böhme¹⁰, V. Boudry²⁷, W. Braunschweig¹, V. Brisson²⁶, H.-B. Bröker²,
 D.P. Brown¹⁰, D. Bruncko¹⁶, F.W. Büsser¹¹, A. Bunyatyan^{12,34}, A. Burrage¹⁸, G. Buschhorn²⁵,
 L. Bystritskaya²³, A.J. Campbell¹⁰, S. Caron¹, F. Cassol-Brunner²², D. Clarke⁵, C. Collard⁴,
 J.G. Contreras^{7,41}, Y.R. Coppens³, J.A. Coughlan⁵, M.-C. Cousinou²², B.E. Cox²¹,
 G. Cozzika⁹, J. Cvach²⁹, J.B. Dainton¹⁸, W.D. Dau¹⁵, K. Daum^{33,39}, M. Davidsson²⁰,
 B. Delcourt²⁶, N. Delerue²², R. Demirchyan³⁴, A. De Roeck^{10,43}, E.A. De Wolf⁴,
 C. Diaconu²², J. Dingfelder¹³, P. Dixon¹⁹, V. Dodonov¹², J.D. Dowell³, A. Droutskoi²³,
 A. Dubak²⁵, C. Duprel², G. Eckerlin¹⁰, D. Eckstein³⁵, V. Efremenko²³, S. Egli³², R. Eichler³²,
 F. Eisele¹³, E. Eisenhandler¹⁹, M. Ellerbrock¹³, E. Elsen¹⁰, M. Erdmann^{10,40,e}, W. Erdmann³⁶,
 P.J.W. Faulkner³, L. Favart⁴, A. Fedotov²³, R. Felst¹⁰, J. Ferencei¹⁰, S. Ferron²⁷,
 M. Fleischer¹⁰, P. Fleischmann¹⁰, Y.H. Fleming³, G. Flügge², A. Fomenko²⁴, I. Foresti³⁷,
 J. Formánek³⁰, G. Franke¹⁰, G. Frising¹, E. Gabathuler¹⁸, K. Gabathuler³², J. Garvey³,
 J. Gassner³², J. Gayler¹⁰, R. Gerhards¹⁰, C. Gerlich¹³, S. Ghazaryan^{4,34}, L. Goerlich⁶,
 N. Gogitidze²⁴, C. Grab³⁶, V. Grabski³⁴, H. Grässler², T. Greenshaw¹⁸, G. Grindhammer²⁵,
 T. Hadig¹³, D. Haidt¹⁰, L. Hajduk⁶, J. Haller¹³, B. Heinemann¹⁸, G. Heinzelmann¹¹,
 R.C.W. Henderson¹⁷, S. Hengstmann³⁷, H. Henschel³⁵, R. Heremans⁴, G. Herrera^{7,44},
 I. Herynek²⁹, M. Hildebrandt³⁷, M. Hilgers³⁶, K.H. Hiller³⁵, J. Hladký²⁹, P. Höting²,
 D. Hoffmann²², R. Horisberger³², A. Hovhannisyan³⁴, S. Hurling¹⁰, M. Ibbotson²¹, Ç. İşsever⁷,
 M. Jacquet²⁶, M. Jaffre²⁶, L. Janauschek²⁵, X. Janssen⁴, V. Jemanov¹¹, L. Jönsson²⁰,
 C. Johnson³, D.P. Johnson⁴, M.A.S. Jones¹⁸, H. Jung^{20,10}, D. Kant¹⁹, M. Kapichine⁸,
 M. Karlsson²⁰, O. Karschnick¹¹, J. Katzy¹⁰, F. Keil¹⁴, N. Keller³⁷, J. Kennedy¹⁸, I.R. Kenyon³,
 C. Kiesling²⁵, P. Kjellberg²⁰, M. Klein³⁵, C. Kleinwort¹⁰, T. Kluge¹, G. Knies¹⁰, B. Koblitz²⁵,
 S.D. Kolya²¹, V. Korbel¹⁰, P. Kostka³⁵, S.K. Kotelnikov²⁴, R. Koutouev¹², A. Koutov⁸,
 J. Kroseberg³⁷, K. Krüger¹⁰, T. Kuhr¹¹, D. Lamb³, M.P.J. Landon¹⁹, W. Lange³⁵,
 T. Laštovička^{35,30}, P. Laycock¹⁸, E. Lebailly²⁶, A. Lebedev²⁴, B. Leißner¹, R. Lemrani¹⁰,
 V. Lendermann¹⁰, S. Levonian¹⁰, B. List³⁶, E. Lobodzinska^{10,6}, B. Lobodzinski^{6,10},
 A. Loginov²³, N. Loktionova²⁴, V. Lubimov²³, S. Lüders³⁷, D. Lüke^{7,10}, L. Lytkin¹²,
 N. Malden²¹, E. Malinovski²⁴, S. Mangano³⁶, R. Maraček²⁵, P. Marage⁴, J. Marks¹³,
 R. Marshall²¹, H.-U. Martyn¹, J. Martyniak⁶, S.J. Maxfield¹⁸, D. Meer³⁶, A. Mehta¹⁸,
 K. Meier¹⁴, A.B. Meyer¹¹, H. Meyer³³, J. Meyer¹⁰, S. Michine²⁴, S. Mikocki⁶, D. Milstead¹⁸,
 S. Mohr dieck¹¹, M.N. Mondragon⁷, F. Moreau²⁷, A. Morozov⁸, J.V. Morris⁵, K. Müller³⁷,
 P. Murín^{16,42}, V. Nagovizin²³, B. Naroska¹¹, J. Naumann⁷, Th. Naumann³⁵, P.R. Newman³,
 F. Niebergall¹¹, C. Niebuhr¹⁰, O. Nix¹⁴, G. Nowak⁶, M. Nozicka³⁰, B. Olivier¹⁰, J.E. Olsson¹⁰,
 D. Ozerov²³, V. Panassik⁸, C. Pascaud²⁶, G.D. Patel¹⁸, M. Peez²², E. Perez⁹, A. Petrukhin³⁵,
 J.P. Phillips¹⁸, D. Pitzl¹⁰, R. Pöschl²⁶, I. Potachnikova¹², B. Povh¹², J. Rauschenberger¹¹,
 P. Reimer²⁹, B. Reisert²⁵, C. Risler²⁵, E. Rizvi³, P. Robmann³⁷, R. Roosen⁴, A. Rostovtsev²³,
 S. Rusakov²⁴, K. Rybicki⁶, D.P.C. Sankey⁵, S. Schätzel¹³, J. Scheins¹⁰, F.-P. Schilling¹⁰,
 P. Schleper¹⁰, D. Schmidt³³, D. Schmidt¹⁰, S. Schmidt²⁵, S. Schmitt¹⁰, M. Schneider²²,
 L. Schoeffel⁹, A. Schöning³⁶, T. Schörner²⁵, V. Schröder¹⁰, H.-C. Schultz-Coulon⁷,
 C. Schwanenberger¹⁰, K. Sedlák²⁹, F. Sefkow³⁷, V. Shekelyan²⁵, I. Sheviakov²⁴,

L.N. Shtarkov²⁴, Y. Sirois²⁷, T. Sloan¹⁷, P. Smirnov²⁴, Y. Soloviev²⁴, D. South²¹, V. Spaskov⁸, A. Specka²⁷, H. Spitzer¹¹, R. Stamen⁷, B. Stella³¹, J. Stiewe¹⁴, I. Strauch¹⁰, U. Straumann³⁷, S. Tchetchelnitski²³, G. Thompson¹⁹, P.D. Thompson³, F. Tomasz¹⁴, D. Traynor¹⁹, P. Truöl³⁷, G. Tsipolitis^{10,38}, I. Tsurin³⁵, J. Turnau⁶, J.E. Turney¹⁹, E. Tzamariudaki²⁵, A. Uraev²³, M. Urban³⁷, A. Usik²⁴, S. Valkár³⁰, A. Valkárová³⁰, C. Vallée²², P. Van Mechelen⁴, A. Vargas Trevino⁷, S. Vassiliev⁸, Y. Vazdik²⁴, C. Veelken¹⁸, A. Vest¹, A. Vichnevski⁸, K. Wacker⁷, J. Wagner¹⁰, R. Wallny³⁷, B. Waugh²¹, G. Weber¹¹, D. Wegener⁷, C. Werner¹³, N. Werner³⁷, M. Wessels¹, G. White¹⁷, S. Wiesand³³, T. Wilksen¹⁰, M. Winde³⁵, G.-G. Winter¹⁰, Ch. Wissing⁷, M. Wobisch¹⁰, E.-E. Woehrling³, E. Wunsch¹⁰, A.C. Wyatt²¹, J. Žáček³⁰, J. Zálešák³⁰, Z. Zhang²⁶, A. Zhokin²³, F. Zomer²⁶, and M. zur Nedden²⁵

¹ *I. Physikalisches Institut der RWTH, Aachen, Germany^a*

² *III. Physikalisches Institut der RWTH, Aachen, Germany^a*

³ *School of Physics and Space Research, University of Birmingham, Birmingham, UK^b*

⁴ *Inter-University Institute for High Energies ULB-VUB, Brussels; Universiteit Antwerpen (UIA), Antwerpen; Belgium^c*

⁵ *Rutherford Appleton Laboratory, Chilton, Didcot, UK^b*

⁶ *Institute for Nuclear Physics, Cracow, Poland^d*

⁷ *Institut für Physik, Universität Dortmund, Dortmund, Germany^a*

⁸ *Joint Institute for Nuclear Research, Dubna, Russia*

⁹ *CEA, DSM/DAPNIA, CE-Saclay, Gif-sur-Yvette, France*

¹⁰ *DESY, Hamburg, Germany*

¹¹ *Institut für Experimentalphysik, Universität Hamburg, Hamburg, Germany^a*

¹² *Max-Planck-Institut für Kernphysik, Heidelberg, Germany*

¹³ *Physikalisches Institut, Universität Heidelberg, Heidelberg, Germany^a*

¹⁴ *Kirchhoff-Institut für Physik, Universität Heidelberg, Heidelberg, Germany^a*

¹⁵ *Institut für experimentelle und Angewandte Physik, Universität Kiel, Kiel, Germany*

¹⁶ *Institute of Experimental Physics, Slovak Academy of Sciences, Košice, Slovak Republic^{e,f}*

¹⁷ *School of Physics and Chemistry, University of Lancaster, Lancaster, UK^b*

¹⁸ *Department of Physics, University of Liverpool, Liverpool, UK^b*

¹⁹ *Queen Mary and Westfield College, London, UK^b*

²⁰ *Physics Department, University of Lund, Lund, Sweden^g*

²¹ *Physics Department, University of Manchester, Manchester, UK^b*

²² *CPPM, CNRS/IN2P3 - Univ Mediterranee, Marseille - France*

²³ *Institute for Theoretical and Experimental Physics, Moscow, Russia^l*

²⁴ *Lebedev Physical Institute, Moscow, Russia^e*

²⁵ *Max-Planck-Institut für Physik, München, Germany*

²⁶ *LAL, Université de Paris-Sud, IN2P3-CNRS, Orsay, France*

²⁷ *LPNHE, Ecole Polytechnique, IN2P3-CNRS, Palaiseau, France*

²⁸ *LPNHE, Universités Paris VI and VII, IN2P3-CNRS, Paris, France*

²⁹ *Institute of Physics, Academy of Sciences of the Czech Republic, Praha, Czech Republic^{e,i}*

³⁰ *Faculty of Mathematics and Physics, Charles University, Praha, Czech Republic^{e,i}*

³¹ *Dipartimento di Fisica Università di Roma Tre and INFN Roma 3, Roma, Italy*

³² *Paul Scherrer Institut, Villigen, Switzerland*

³³ *Fachbereich Physik, Bergische Universität Gesamthochschule Wuppertal, Wuppertal, Germany*

³⁴ *Yerevan Physics Institute, Yerevan, Armenia*

³⁵ *DESY, Zeuthen, Germany*

³⁶ *Institut für Teilchenphysik, ETH, Zürich, Switzerland^j*

³⁷ *Physik-Institut der Universität Zürich, Zürich, Switzerland^j*

³⁸ *Also at Physics Department, National Technical University, Zografou Campus, GR-15773 Athens, Greece*

³⁹ *Also at Rechenzentrum, Bergische Universität Gesamthochschule Wuppertal, Germany*

⁴⁰ *Also at Institut für Experimentelle Kernphysik, Universität Karlsruhe, Karlsruhe, Germany*

⁴¹ *Also at Dept. Fis. Ap. CINVESTAV, Mérida, Yucatán, México^k*

⁴² *Also at University of P.J. Šafárik, Košice, Slovak Republic*

⁴³ *Also at CERN, Geneva, Switzerland*

⁴⁴ *Also at Dept. Fis. CINVESTAV, México City, México^k*

^a *Supported by the Bundesministerium für Bildung und Forschung, FRG, under contract numbers 05 H1 1GUA /1, 05 H1 1PAA /1, 05 H1 1PAB /9, 05 H1 1PEA /6, 05 H1 1VHA /7 and 05 H1 1VHB /5*

^b *Supported by the UK Particle Physics and Astronomy Research Council, and formerly by the UK Science and Engineering Research Council*

^c *Supported by FNRS-FWO-Vlaanderen, IISN-IIKW and IWT*

^d *Partially Supported by the Polish State Committee for Scientific Research, grant no. 2P0310318 and SPUB/DESY/P03/DZ-1/99 and by the German Bundesministerium für Bildung und Forschung*

^e *Supported by the Deutsche Forschungsgemeinschaft*

^f *Supported by VEGA SR grant no. 2/1169/2001*

^g *Supported by the Swedish Natural Science Research Council*

ⁱ *Supported by the Ministry of Education of the Czech Republic under the projects INGO-LA116/2000 and LN00A006, by GAUK grant no 173/2000*

^j *Supported by the Swiss National Science Foundation*

^k *Supported by CONACyT*

^l *Partially Supported by Russian Foundation for Basic Research, grant no. 00-15-96584*

Among the unexplained features of the Standard Model (SM) of particle physics is the existence of three distinct generations of fermions and the hierarchy of their masses. One possible explanation for this is fermion substructure, with the constituents of the known fermions being strongly bound together by a new, as yet undiscovered force [1, 2]. A natural consequence of these models would be the existence of excited states of the known leptons and quarks. Assuming a compositeness scale in the TeV region, one would naively expect that the excited fermions have masses in the same energy region. However, the dynamics of the constituent level are unknown, so the lowest excited states could have masses of the order of only a few hundred GeV. Electron¹-proton interactions at very high energies provide an excellent environment in which to search for excited fermions of the first generation. These excited electrons (e^*) could be singly produced through t -channel γ and Z boson exchange. Their production cross-section and partial decay widths have been calculated using an effective Lagrangian [3, 4] which depends on a compositeness mass scale Λ and on weight factors f and f' describing the relative coupling strengths of the excited lepton to the $SU(2)_L$ and $U(1)_Y$ gauge bosons, respectively. In this model the excited electron can decay to an electron or a neutrino via the radiation of a gauge boson (γ , W , Z) with branching ratios determined by the e^* mass and the coupling parameters f and f' . In most analyses [5–7] the assumption is made that these coupling parameters are of comparable strength and only the relationships $f = +f'$ or $f = -f'$ are considered. If a relationship between f and f' is assumed, the production cross-section and partial decay widths depend on two parameters only, namely the e^* mass and the ratio f/Λ .

In this paper excited electrons are searched for in three samples of data taken by the H1 experiment from 1994 to 2000 with a total integrated luminosity of 120 pb^{-1} . The first sample consists of e^+p data accumulated from 1994 to 1997 at positron and proton beam energies of 27.5 GeV and 820 GeV respectively, and corresponds to an integrated luminosity of 37 pb^{-1} . A search for excited electrons using this sample of data has been previously published [8]. The strategy for the selection of events has been modified from the procedures described in [8] to optimize the sensitivity to higher e^* masses. The two other samples were taken from 1998 to 2000 with an electron or positron beam energy of 27.5 GeV and a proton beam energy of 920 GeV. The integrated luminosities of the e^-p and e^+p samples are 15 pb^{-1} and 68 pb^{-1} , respectively. Compared to previous H1 results [8] the analysis presented here benefits from an increase in luminosity by a factor of more than three and an increase of the centre-of-mass energy from 300 GeV to 318 GeV.

We search for all electroweak decays $e^* \rightarrow e\gamma$, $e^* \rightarrow eZ$ and $e^* \rightarrow \nu W$, considering the subsequent Z and W hadronic decay modes only. This leads to final states containing an electron and a photon, an electron and jets or jets with missing transverse energy induced by the neutrinos escaping from the detector. The Standard Model backgrounds which could mimic such signatures are neutral current Deep Inelastic Scattering (NC DIS), charged current Deep Inelastic Scattering (CC DIS), QED Compton scattering (or Wide Angle Bremsstrahlung WAB), photoproduction processes (γp) and lepton pair production via the two photon fusion process ($\gamma\gamma$).

¹The term “electron” is used generically to refer to both electrons and positrons.

The determination of the contribution of NC DIS processes is performed using two Monte Carlo samples which employ different models of QCD radiation. The first was produced with the DJANGO [9] event generator which includes QED first order radiative corrections based on HERACLES [10]. QCD radiation is implemented using ARIADNE [11] based on the Colour Dipole Model [12]. This sample, with an integrated luminosity of more than 10 times the experimental luminosity, is chosen to estimate the NC DIS contribution in the $e^* \rightarrow e\gamma$ analysis. The second sample was generated with the program RAPGAP [13], in which QED first order radiative corrections are implemented as described above. RAPGAP includes the leading order QCD matrix element and higher order radiative corrections are modelled by leading-log parton showers. This sample is used to determine potential NC DIS background in the $e^* \rightarrow \nu W_{\rightarrow q\bar{q}}$ and $e^* \rightarrow eZ_{\rightarrow q\bar{q}}$ searches, as RAPGAP describes better this particular phase space domain [8]. For both samples the parton densities in the proton are taken from the MRST [14] parametrization which includes constraints from DIS measurements at HERA up to squared momentum transfers $Q^2 = 5000 \text{ GeV}^2$ [15–18]. Hadronisation is performed in the Lund string fragmentation scheme using JETSET [19]. The modelling of the CC DIS process is performed using the DJANGO program with MRST structure functions. While inelastic WAB is treated using the DJANGO generator, elastic and quasi-elastic WAB is simulated with the WABGEN [20] event generator. Direct and resolved γp processes including prompt photon production are generated with the PYTHIA [21] event generator. Finally the $\gamma\gamma$ process is produced using the LPAIR generator [22].

For the calculation of the e^* production cross-section and to determine the efficiencies, events have been generated with the COMPOS [23] generator based on the cross-section formulae given in reference [3] and the partial decay widths stated in reference [4]. Initial state radiation of a photon from the incoming electron is included. This generator uses the narrow width approximation (NWA) for the calculation of the production cross section and takes into account the natural width for the e^* decay. For all values of f/Λ relevant to this analysis this assumption is valid even at high e^* masses where the natural width of the e^* is of the order of the experimental resolution. To give an example, for $M_{e^*} = 250 \text{ GeV}$ this resolution is equal to 7 GeV, 10 GeV, and 12 GeV for the $e\gamma$, eZ and νW decay modes, respectively. All Monte Carlo samples are subjected to a detailed simulation of the response of the H1 detector.

The detector components of the H1 experiment [24] most relevant for this analysis are briefly described in the following. Surrounding the interaction region is a system of drift and proportional chambers which covers the polar angle² range $7^\circ < \theta < 176^\circ$. The tracking system is surrounded by a finely segmented liquid argon (LAr) calorimeter covering the polar angle range $4^\circ < \theta < 154^\circ$ [25] with energy resolutions of $\sigma_E/E \simeq 12\%/\sqrt{E} \oplus 1\%$ for electrons and $\sigma_E/E \simeq 50\%/\sqrt{E} \oplus 2\%$ for hadrons, obtained in test beam measurements [26, 27]. The tracking system and calorimeters are surrounded by a superconducting solenoid and an iron yoke instrumented with streamer tubes. Backgrounds not related to e^+p or e^-p collisions are rejected by requiring that a primary interaction vertex be reconstructed within $\pm 35 \text{ cm}$ of the nominal vertex position, by using filters based on the event topology and by requiring an event time which is consistent with the interaction time. Electromagnetic clusters are required to have

²The polar angle θ is measured with respect to the proton beam direction ($+z$).

more than 95% of their energy in the electromagnetic part of the calorimeter and to be isolated from other particles [28]. They are further differentiated into electron and photon candidates using the tracking chambers. Jets with a minimum transverse momentum of 5 GeV are reconstructed from the hadronic final state using a cone algorithm adapted from the LUCCELL scheme in the JETSET package [19]. Missing transverse energy (E_t^{miss}) is reconstructed using the vector sum of energy depositions in the calorimeter cells. The analysis presented in this paper is described extensively in [29].

The $e^* \rightarrow e\gamma$ channel is characterized by two electromagnetic clusters in the final state. The main sources of background are the WAB process, NC DIS with photon radiation or a high energy π^0 in a jet and the production of electron pairs via $\gamma\gamma$ fusion. Candidate events are selected with two electromagnetic clusters in the LAr calorimeter of transverse energy greater than 20 GeV and 15 GeV, respectively, and with a polar angle between 0.1 and 2.2 radians. The sum of the energies of the two clusters has to be greater than 100 GeV. If this sum is below 200 GeV, the background is further suppressed by rejecting events with a total transverse energy of the two electromagnetic clusters lower than 75 GeV or with more than two tracks spatially associated to one of the clusters. The numbers of events passing the analysis cuts for the SM background processes and for the data in each of the three samples are given in Table 1. About half of the background originates from NC DIS events with most of the remainder being due to WAB events. The efficiency for selecting the signal varies from 85% for an e^* mass of 150 GeV to 72% for an e^* mass of 250 GeV. As in all other channels the efficiencies are derived using samples of 1000 e^* events generated at different e^* masses. The various sources of systematic error are discussed later. Distributions of the invariant mass of the candidate electron-photon pairs of the three data samples together and for the SM expectation are shown in Fig. 1a.

Sample	e^+p 820 GeV		e^-p 920 GeV		e^+p 920 GeV	
	Data	SM background	Data	SM background	Data	SM background
$e^* \rightarrow e\gamma$	8	$7.2 \pm 1.0 \pm 0.1$	4	$4.0 \pm 0.7 \pm 0.2$	12	$15.6 \pm 1.7 \pm 0.4$
$e^* \rightarrow eZ \rightarrow q\bar{q}$	6	$7.1 \pm 2.1 \pm 2.8$	4	$5.6 \pm 0.4 \pm 1.2$	31	$25.3 \pm 1.9 \pm 5.5$
$e^* \rightarrow \nu W \rightarrow q\bar{q}$	2	$2.4 \pm 0.2 \pm 0.7$	5	$3.9 \pm 0.2 \pm 0.7$	8	$6.1 \pm 0.4 \pm 1.5$

Table 1: Number of candidate events observed in the three decay channels with the corresponding SM expectation and the uncertainties on the expectation (statistical and systematic error).

The $e^* \rightarrow eZ \rightarrow q\bar{q}$ channel is characterized by an electromagnetic cluster with an associated track and two high transverse energy jets. The analysis for this channel uses a sample of events with at least two jets with a transverse energy above 17 GeV and 16 GeV, respectively, and an electron candidate with a transverse energy $E_t^e > 20$ GeV. These two jets and the electron must have polar angles smaller than 2.2 radians. Furthermore, to avoid possible double counting of events from the $e^* \rightarrow e\gamma$ channel, events with two electromagnetic clusters with transverse energies above 10 GeV and a total energy of the two clusters greater than 100 GeV are removed. The main SM contribution is NC DIS as photoproduction events do not yield a significant rate of electron candidates with large E_t^e . For $20 \text{ GeV} < E_t^e < 65 \text{ GeV}$, a cut is made on the

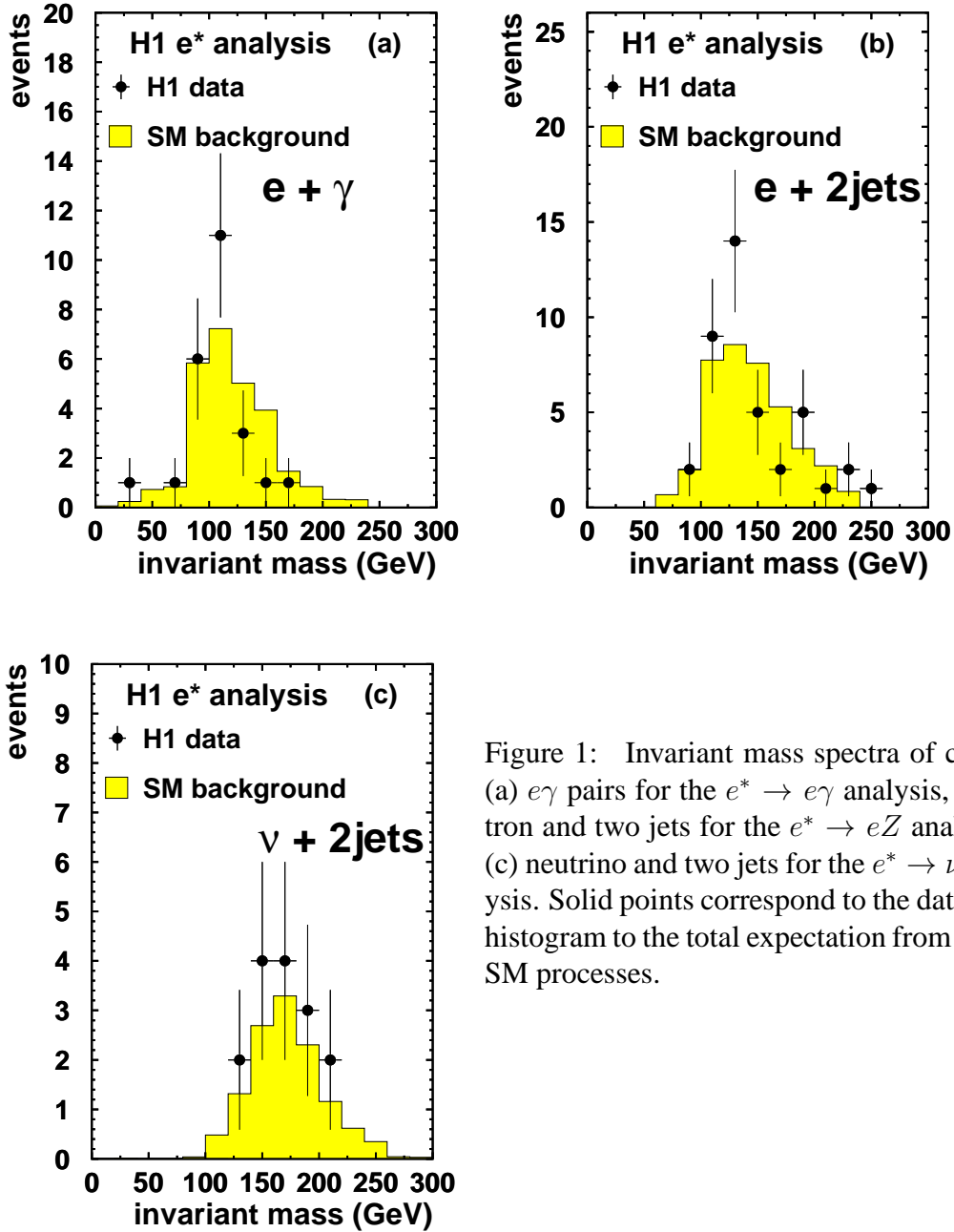


Figure 1: Invariant mass spectra of candidate (a) $e\gamma$ pairs for the $e^* \rightarrow e\gamma$ analysis, (b) electron and two jets for the $e^* \rightarrow eZ$ analysis and (c) neutrino and two jets for the $e^* \rightarrow \nu W$ analysis. Solid points correspond to the data and the histogram to the total expectation from different SM processes.

electron polar angle. This ranges from $\theta_e < 1.35$ for $E_t^e = 20$ GeV to $\theta_e < 2.2$ radians for $E_t^e = 65$ GeV and depends linearly on E_t^e . The dijet invariant mass has to be in the range $-15 < M_{jj} - M_Z < 7$ GeV. If there are more than two jets, the pair with invariant mass closest to the nominal Z boson mass is chosen as the Z candidate. The two jets chosen are ordered such that $E_t^{jet1} > E_t^{jet2}$. In many SM events the direction of jet 2 is close to the proton direction. To ensure that this jet is well measured, an additional cut on its polar angle, $\theta^{jet2} > 0.2$ radians,

is applied if its transverse momentum is lower than 30 GeV. For an electron transverse energy $65 \text{ GeV} < E_t^e < 85 \text{ GeV}$ two jets with an invariant mass $M_{jj} > M_Z - 30 \text{ GeV}$ are required. At very high transverse energy, $E_t^e > 85 \text{ GeV}$, the contribution from NC DIS is very low and no further cuts on M_{jj} are needed. The number of events which remain in the data after these cuts are summarized in Table 1 and compared with the expected SM contribution (mostly NC DIS events). The efficiency for selecting the signal varies from 44% for an e^* mass of 150 GeV to 62% for an e^* mass of 250 GeV. Distributions of the invariant mass of the electron and the two jets are shown in Fig. 1b for data and for the SM expectation.

The $e^* \rightarrow \nu W_{\rightarrow q\bar{q}}$ channel is characterized by two jets and missing transverse energy E_t^{miss} . The main background originates from CC DIS events with a moderate contribution from photo-production, whereas the NC DIS contribution is suppressed for large E_t^{miss} . The analysis starts from a sample of events with at least two jets with transverse energies above 17 GeV and 16 GeV, missing transverse energy $E_t^{miss} > 20 \text{ GeV}$ and no isolated electromagnetic cluster with transverse energy above 10 GeV. The jets must have a polar angle below 2.2 radians. Jets in which the most energetic track enters the boundary region between two calorimeter modules and central jets ($\theta > 0.5$ radians) are required to contain more than two tracks. This cut removes NC DIS events in which the scattered electron is misidentified as a jet. Only events with $S = \frac{V_{ap}}{V_p} < 0.1$ are accepted, where V_{ap} and V_p are, respectively, the projections of the transverse energy flow antiparallel and parallel to the transverse momentum vector of the hadronic system. This cut rejects γp background for which S is close to 1, whereas for the signal S is close to 0. At very high missing transverse energy, $E_t^{miss} > 65 \text{ GeV}$, the background is low and no further cuts are applied. The dijet-pair with invariant mass closest to the nominal W boson mass is chosen as the W candidate provided its mass is in the range $-15 \text{ GeV} < M_W - M_{jj} < 15 \text{ GeV}$. The number of events which remain in the data after these cuts is summarized in Table 1. Also given is the expected SM contribution (CC DIS events) for each sample. The efficiency for selecting the signal varies from 30% for an e^* mass of 150 GeV to 52% for an e^* mass of 250 GeV. Distributions of the invariant mass of the reconstructed neutrino and the two jets are shown in Fig. 1c for data and for the SM expectation.

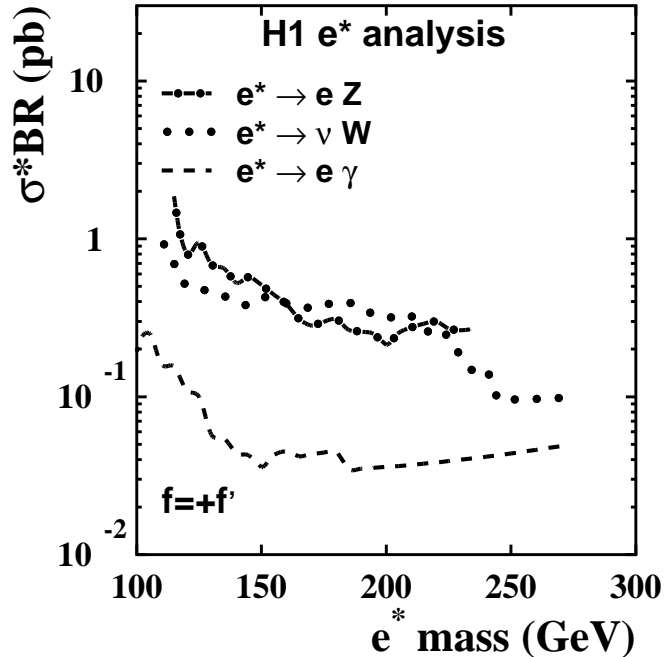
Contributions to the systematic error of the SM expectation come from the uncertainty on the absolute energy scale of the calorimeter and missing higher order corrections in the event generators which are used for the background estimation. The uncertainties of the electromagnetic energy scale vary from 0.7% in the central part of the detector to 3% in the forward region. For the hadronic energy scale an uncertainty of 4% is assigned. For the $e^* \rightarrow \nu W_{\rightarrow q\bar{q}}$ and $e^* \rightarrow e Z_{\rightarrow q\bar{q}}$ channels the SM expectation is varied by 15% to account for differences observed in particular in two jet production between perturbative calculations of order $O(\alpha_s^2)$ [30–32] and the parton shower approach. The statistical error of the Monte Carlo samples is taken into account as a systematic error on the efficiencies. Finally, the luminosity measurement leads to a normalization uncertainty of 1.5%.

In all three search channels the numbers of observed and expected events are in good agreement. Upper limits on the cross section and on the coupling f/Λ are thus derived as a function of the e^* mass at 95% confidence level as described in [8] following the Bayesian approach [33,34]. For a given e^* mass, the limits are obtained by counting the number of observed and expected

events in a mass interval that varies with the width of the expected signal. At $M_{e^*} = 150$ GeV, a width of the mass interval of 30 GeV is chosen for the $e^* \rightarrow e\gamma$ decay mode and 60 GeV is chosen for the decay channels with two jets. Systematic uncertainties are taken into account as in [8]. The limits on the product of the e^* production cross-section and the decay branching ratio are shown in Fig. 2. As stated in the introduction, most experiments give f/Λ limits under the assumptions $f = +f'$ and $f = -f'$. The H1 limits for each decay channel and after combination of all decay channels are given as a function of the e^* mass in Fig. 3a, for the assumption $f = +f'$. With this hypothesis the main contribution comes from the $e^* \rightarrow e\gamma$ channel. The values of the limits for f/Λ vary between 5×10^{-4} and 10^{-2} GeV^{-1} for an e^* mass ranging from 130 GeV to 275 GeV. These results improve significantly the previously published H1 limits for e^+p [8] collisions.

The LEP experiments [5, 6] and the ZEUS collaboration [7] have also reported on excited electron searches. Their limits are shown in Fig. 3b. The LEP 2 experiments have shown results in two mass domains. In direct searches for excited electrons limits up to a mass of about 200 GeV are given. Above 200 GeV their results are derived from indirect searches only. The H1 limit extends the excluded region to higher masses than reached in previous direct searches.

Figure 2: Upper limits at 95% confidence level on the product of the production cross-section σ and the decay branching ratio BR for excited electrons e^* in the various electroweak decay channels, $e^* \rightarrow e\gamma$ (dashed line), $e^* \rightarrow eZ \rightarrow q\bar{q}$ (dotted-dashed line) and $e^* \rightarrow \nu W \rightarrow q\bar{q}$ (dotted line) as a function of the excited electron mass. The signal efficiencies used to compute these limits have been determined with events generated under the assumption $f = +f'$.



More generally, limits on f/Λ as a function of f'/f are shown in Fig. 4 for three e^* masses (150, 200 and 250 GeV). It is worth noting that excited electrons have vanishing electromagnetic coupling for $f = -f'$. In this case the e^* is produced through pure Z boson exchange. As a consequence the production cross-section for excited electrons at HERA is much smaller in the $f = -f'$ case than in the $f = +f'$ case. For e^* masses between 150 and 250 GeV the ratio

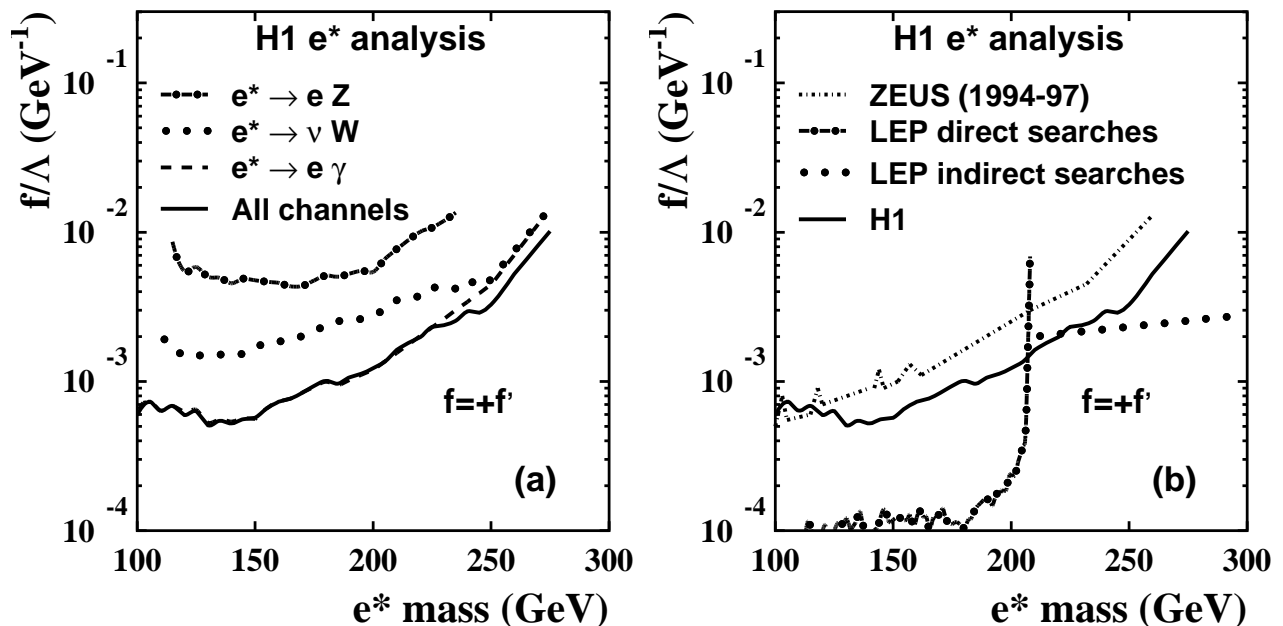


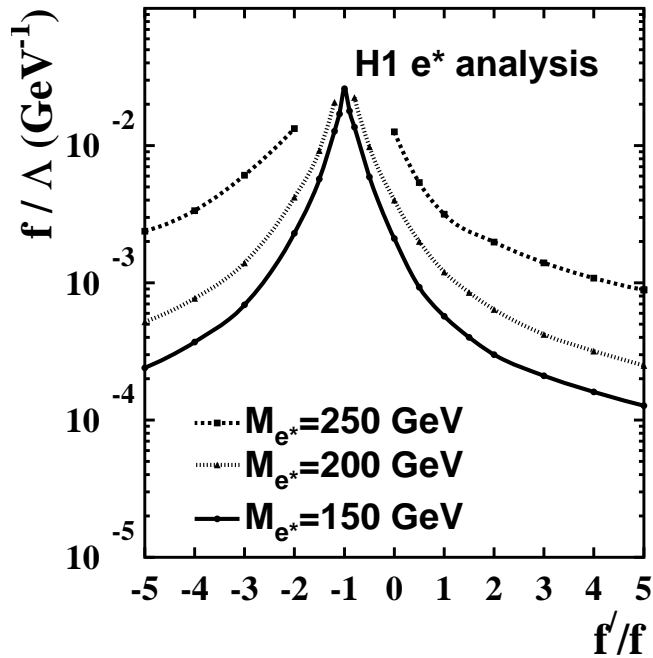
Figure 3: Exclusion limits on the coupling f/Λ at 95% confidence level as a function of the mass of excited electrons with the assumption $f = +f'$. (a) Limit for each decay channel $e^* \rightarrow e\gamma$ (dashed line), $e^* \rightarrow eZ_{\rightarrow q\bar{q}}$ (thick dotted-dashed line), $e^* \rightarrow \nu W_{\rightarrow q\bar{q}}$ (dotted line) and for the combination of the three channels (full line). It must be noted that a part of the data included in the present result were used to obtain the previous H1 limit [8]. (b) Comparison of this analysis with ZEUS results [7] (dashed line) and LEP 2 results on direct searches [5] (dotted-dashed line) and on indirect searches [6] (dotted line).

of the cross-sections for $f = +f'$ and $f = -f'$ varies between 170 and 900. For high e^* masses and some values of the couplings, no limits are given because the natural width of the e^* would become extremely large.

In summary, a search for excited electron production was performed using all the e^+p and e^-p data accumulated by H1 between 1994 and 2000. No indication of a signal was found. New limits have been established as a function of the couplings and the excited electron mass for the conventional relationship between the couplings $f = +f'$. The dependence of the f/Λ limit on the ratio f'/f has been shown for the first time at HERA. The data presented here restrict excited electrons to higher mass values than has been possible previously in direct searches.

We are grateful to the HERA machine group whose outstanding efforts have made and continue to make this experiment possible. We thank the engineers and technicians for their work in constructing and now maintaining the H1 detector, our funding agencies for financial support, the DESY technical staff for continual assistance and the DESY directorate for the hospitality which they extend to the non-DESY members of the collaboration.

Figure 4: Exclusion limits on the coupling f/Λ at 95% confidence level as a function of the ratio f'/f for three different masses of the e^* : 150 GeV (full line), 200 GeV (dotted line) and 250 GeV (dashed line).



References

- [1] H. Harari, Phys. Rep. **104** (1984) 159.
- [2] F. Boudjema, A. Djouadi and J. L. Kneur, Z. Phys. C **57** (1993) 425.
- [3] K. Hagiwara, D. Zeppenfeld and S. Komamiya, Z. Phys. C **29** (1985) 115.
- [4] U. Baur, M. Spira and P. M. Zerwas, Phys. Rev. D **42** (1990) 815.
- [5] G. Abbiendi *et al.* [OPAL Collaboration], CERN-EP/2002-043, arXiv:hep-ex/0206061. Submitted to Phys. Lett. B
- [6] P. Abreu *et al.* [DELPHI Collaboration], Eur. Phys. J. C **8** (1999) 41 [hep-ex/9811005].
- [7] S. Chekanov *et al.* [ZEUS Collaboration], DESY-01-132 arXiv:hep-ex/0109018.
- [8] C. Adloff *et al.*, [H1 Collaboration], Eur. Phys. J. C **17** (2000) 567 [hep-ex/0007035].
- [9] G. A. Schuler and H. Spiesberger, in: Proceedings of *Physics at HERA*, Hamburg 1991, Vol. 3, pp. 1419-1432.
- [10] A. Kwiatkowski, H. Spiesberger and H. J. Möhring, Comput. Phys. Commun. **69** (1992) 155.

- [11] L. Lönnblad, *Comput. Phys. Commun.* **71** (1992) 15.
- [12] B. Andersson, G. Gustafson, L. Lönnblad and U. Pettersson, *Z. Phys. C* **43** (1989) 625.
- [13] H. Jung, *Comput. Phys. Commun.* **86** (1995) 147.
- [14] A. D. Martin, R. G. Roberts, W. J. Stirling and R. S. Thorne, *Eur. Phys. J. C* **4** (1998) 463. [hep-ph/9803445].
- [15] S. Aid *et al.*, [H1 Collaboration], *Nucl. Phys. B* **470** (1996) 3 [hep-ex/9603004].
- [16] C. Adloff *et al.*, [H1 Collaboration], *Nucl. Phys. B* **497** (1997) 3 [hep-ex/9703012].
- [17] M. Derrick *et al.*, [ZEUS Collaboration], *Z. Phys. C* **69** (1996) 607 [hep-ex/9510009].
- [18] M. Derrick *et al.*, [ZEUS Collaboration], *Z. Phys. C* **72** (1996) 399 [hep-ex/9607002].
- [19] T. Sjöstrand, hep-ph/9508391, LU-TP-95-20, CERN-TH-7112-93-REV, August 1995.
- [20] C. Berger and P. Kandel, Proceedings of the Workshop *Monte Carlo generators for HERA Physics*, Hamburg 1998-1999, pp. 596-600, [hep-ph/9906541].
- [21] T. Sjöstrand, *Comput. Phys. Commun.* **82** (1994) 74.
- [22] S. P. Baranov, O. Dünger, H. Shooshtari and J. A. Vermaseren, Proceedings of *Physics at HERA*, Hamburg 1991, vol. 3, pp. 1478-1482.
- [23] T. Köhler, Proceedings of *Physics at HERA*, Hamburg 1991, vol. 3, pp. 1526-1541.
- [24] I. Abt *et al.*, [H1 Collaboration], *Nucl. Instrum. Meth. A* **386** (1997) 310; *ibid.* 348.
- [25] B. Andrieu *et al.*, [H1 Calorimeter Group], *Nucl. Instrum. Meth. A* **336** (1993) 460.
- [26] B. Andrieu *et al.*, [H1 Calorimeter Group], *Nucl. Instrum. Meth. A* **350** (1994) 57.
- [27] B. Andrieu *et al.* [H1 Calorimeter Group], *Nucl. Instrum. Meth. A* **336** (1993) 499.
- [28] A. Schöning, *Untersuchung von Prozessen mit virtuellen und reellen W^\pm -Bosonen am H1-Detektor bei HERA*, Ph.D. Thesis, University of Hamburg, 1996. https://www-h1.desy.de/publications/theses_list.html
- [29] N. Delerue, *Recherche de leptons excités dans les données de l'expérience H1 auprès du collisionneur HERA*, Thèse de doctorat de l'Université de la Méditerranée, 2002. https://www-h1.desy.de/publications/theses_list.html
- [30] T. Carli, Proceedings of the Workshop *Monte Carlo generators for HERA Physics 1998-1999*, pp. 185-194, [hep-ph/9906541].
- [31] P. Bate, *High Transverse Momentum 2-jet and 3-jet Cross-section Measurements in Photoproduction*, Ph.D. Thesis, University of Manchester, 1999.

[32] C. Adloff *et al.*, [H1 Collaboration], Phys. Lett. B **515** (2001) 17.

[33] R. M. Barnett *et al.*, Particle Data Group, Phys. Rev. D **54** (1996) 1.

[34] O. Helene, Nucl. Instrum. Meth. A **228** (1984) 120.